Observation of an unexpected third receptor molecule in the crystal structure of human interferon-γ receptor complex

DJ Thiel[1], M-H le Du[1†], RL Walter[1‡], A D'Arcy[2], C Chène[2], M Fountoulakis[2], G Garotta[2§], FK Winkler[2] and SE Ealick[3*]

Background: Molecular interactions among cytokines and cytokine receptors form the basis of many cell-signaling pathways relevant to immune function. Interferon-γ (IFN-γ) signals through a multimeric receptor complex consisting of two different but structurally related transmembrane chains: the high-affinity receptor-binding subunit (IFN-γRα) and a species-specific accessory factor (AF-1 or IFN-γRβ). In the signaling complex, the two receptors probably interact with one another through their extracellular domains. Understanding the atomic interactions of signaling complexes enhances the ability to control and alter cell signaling and also provides a greater understanding of basic biochemical processes.

Results: The crystal structure of the complex of human IFN-γ with the soluble, glycosylated extracellular part of IFN-γRα has been determined at 2.9 Å resolution using multiwavelength anomalous diffraction methods. In addition to the expected 2:1 complex, the crystal structure reveals the presence of a third receptor molecule not directly associated with the IFN-γ dimer. Two distinct intermolecular contacts, involving the edge strands of the C-terminal domains, are observed between this extra receptor and the 2:1 receptor–ligand complex thereby forming a 3:1 complex.

Conclusions: The observed interactions in the 2:1 complex of the high-affinity cell-surface receptor with the IFN-γ cytokine are similar to those seen in a previously reported structure where the receptor chains were not glycosylated. The formation of β-sheet packing interactions between pairs of IFN-γRα receptors in these crystals suggests a possible model for receptor oligomerization of Rα and the structurally homologous Rβ receptors in the fully active IFN-γ signaling complex.

Addresses: [1]Section of Biochemistry, Molecular & Cell Biology, Cornell University, Ithaca, NY 14853, USA, [2]Preclinical Research, F. Hoffmann-La Roche Ltd., Basel, Switzerland and [3]Department of Chemistry and Chemical Biology, Cornell University, Ithaca, NY 14853, USA.

Present addresses: [†]Departement d'Ingéniérie et d'Etude des Protéines, Bat 152, CEA-Saclay, 91191 Gif sur Yvette, France, [‡]Proctor and Gamble, Miami Valley Labs, PO Box 538707 Cincinnati, OH 45253, USA and [§]Human Genome Sciences, Rockville, MD 20850-3338, USA.

*Corresponding author.
E-mail: see3@cornell.edu

Key words: interferon-γ, membrane receptor, X-ray structure

Received: **21 June 2000**
Accepted: **10 July 2000**

Published: **11 August 2000**

Structure 2000, **8**:927–936

0969-2126/00/$ – see front matter

Introduction

Receptor oligomerization is necessary in the signaling cascades of nearly all known members of the cytokine receptor superfamily. This superfamily is composed of two subdivisions, the class 1 and the class 2 cytokine receptors, which share a molecular architecture consisting of a ligand-binding extracellular domain, a single transmembrane region and a cytoplasmic domain [1]. Members of the class 1 subdivision include the growth hormone (GH) receptor, the prolactin receptor, the erythropoietin receptor, the granulocyte and granulocyte/macrophage colony-stimulating factor receptors, receptors for various interleukins, and the receptor for ciliary neurotrophic factor. Members of the class 2 subdivision include the two interferon-γ (IFN-γ) receptor chains (Rα and Rβ), the two chains of the IFN-α/β receptor, the interleukin-10 receptor, tissue factor, and the receptor-like molecule CRF2–4. The distinction between the two cytokine receptor classes is made on the basis of differences within the extracellular domains. Class 2 receptors lack the sequence WSXWS (in single-letter amino acid code) found in the C-terminal domain of the extracellular portion of class 1 receptors. In addition, two pairs of conserved cysteine residues absent in the class 1 receptors are found in the extracellular domains of class 2 cytokine receptors [1]. In the case of IFN-γ, the high-affinity cell-surface receptor α chain, IFN-γRα, is known to initiate the signal transduction pathway by binding the IFN-γ homodimer ($K_d = 10^{-10}$ M) with a 2:1 stoichiometry [2]. A second cell-surface receptor, the species-specific β chain IFN-γRβ, also referred to as accessory factor 1 (AF-1), is known to associate with the 2:1 complex to form the active signaling complex with a 2:2:1 stoichiometry [2,3].

In the cytokine signaling pathways, initial receptor oligomerization occurs upon the binding of the signaling ligand to the extracellular domain of the receptor molecule specific to that cytokine. Further oligomerization of additional species-specific receptors is essential in the case of IFN-γ and other receptors. Because the intracellular regions of these receptor molecules lack any common structural motif, the extracellular regions are probably involved in the mechanism of receptor oligomerization in addition to the

binding of the ligand. On the basis of sequence analysis of the known members of the cytokine receptor superfamily, it was proposed that all members of this superfamily exhibit a tandem set of fibronectin type-III domains within their extracellular domains [1]. Because fibronectin type-III structures are typically found in cell-surface molecules with adhesive functions, this finding established a link between cytokine receptors and cell adhesive molecules. In light of this link, investigations of receptor–receptor interactions of the superfamily are likely to provide additional understanding of signal transduction by elucidating the mechanisms and roles of receptor oligomerization.

Crystal structure data depicting the generally weak receptor–receptor interactions in atomic detail are limited. Recently, ligand-induced, receptor–receptor dimeric interactions have been suggested as relevant in the mediation of signal transduction in T cells [4]. The soluble portion of human CD4 (sCD4), a receptor molecule with structural similarity to the cytokine receptor family, was found to form dimers when crystallized in the absence of glycosylation. The dimerization was suggested to play a role in signal transduction during antigen recognition through the cytoplasmic association of CD4 with the lymphocyte kinase Lck. In the case of CD4, the receptor–receptor interaction is induced by the association with a T cell and not through binding of a soluble, secreted molecule.

In contrast, several structures of the typically tight binding complexes between members of the cytokine receptor superfamily and their natural ligands have been determined. The human GH receptor complex, in which two extracellular receptor fragments interact asymmetrically with the GH ligand, was the first crystal structure of a cytokine receptor complex [5]. Similar studies have now provided detailed structural information on a number of such systems and have illustrated considerable structural variety in the receptor–ligand interactions [6–12]. Of most relevance to this study, the crystal structure of a 2:1 complex between soluble non-glycosylated human IFN-γRα (sIFN-γRα) and IFN-γ with two receptor molecules bound to the dimeric ligand has been reported by Walter *et al.* [7] and, more recently, a 1:1 crystal structure of human sIFN-γRα bound to a mutant monomeric form of IFN-γ [13] (AA Kossiakoff, personal communication) has been determined. Except for one of the interleukin-1 structures [11] where the first carbohydrate units at the glycosylation sites were observed in the electron-density maps, none of these receptor fragments were expressed with glycosylation, and virtually no structural data exist regarding the role of glycosylation in these receptor complexes.

Here, we report a crystal structure containing a complex of two glycosylated sIFN-γRα molecules and one non-glycosylated IFN-γΔ10 dimer plus a third unexpected glycosylated sIFN-γRα molecule. The notation Δ10 indicates a ten-residue deletion of the C terminus of each monomer, hereafter referred to as IFN-γ. The C-terminal truncation slightly enhances receptor affinity [14]. In this crystal structure, the IFN-γ dimer binds two of the glycosylated sIFN-γRα molecules, as previously reported for the 2:1 non-glycosylated complex [7]. The third sIFN-γRα molecule makes two distinct contacts with the receptor chains of the 2:1 complex. Previous studies have demonstrated multisubunit complex formation between IFN-γ and the two receptor chains, Rα and Rβ, both in solution and at the cell surface [2]. These studies suggest that the 2:1 sIFN-γRα–IFN-γ complex associates with two chains of the IFN-γRβ receptor. Because of the significant structural similarity between the Rα and Rβ proteins [15], the receptor–receptor interactions reported here have been examined as models of how the IFN-γRβ receptor might associate with the 2:1 complex to form the activated complex necessary for signaling.

Results and discussion

Structure determination by MAD phasing

Crystals of the sIFN-γRα–IFN-γ complex were variable in quality and rarely diffracted beyond 3.8 Å [16]. In addition, attempts to produce heavy-atom derivatives were unsuccessful. Therefore, conventional heavy-atom methods for structure determination were abandoned and multiwavelength anomalous diffraction (MAD) phasing was used. Selenium incorporation into the complex was accomplished by substituting the methionine residues of only the IFN-γ dimer with selenomethionine (SeMet) and binding this SeMet-substituted IFN-γ to the unsubstituted, glycosylated sIFN-γRα [16]. Compared to human IFN-γ, *Escherichia coli*-derived IFN-γ contains an extra methionine at the N terminus of each monomer, which was found to be disordered in the complex. Hence, phase determination for the 120 kDa complex utilized only six selenium sites.

The crystal structure was determined by MAD phasing using 3.8 Å data merged from four SeMet crystals and extended to 2.9 Å using native data from one crystal. Synchrotron radiation and charge-coupled device (CCD)-based X-ray detectors were utilized for all data collection. The structure was refined to an R factor of 23.7% (R_{free} = 30.2%) using diffraction data from 6.0 Å to 2.9 Å. Results of the refinement are shown in Table 1; the final model has good stereochemistry. The Ramachandran plot shows none of the amino acid residues of the IFN-γ in the disallowed regions and only one sIFN-γRα residue, Val206, in the disallowed region for all three receptors.

The structure determination of this sIFN-γRα–IFN-γ complex demonstrates the capability of the MAD phasing technique applied to large macromolecular assemblies, even when the anomalous signal is weak. Although the quality of the crystals was poor, resulting in very weak diffraction, the 120 kDa complex is one of the largest

Table 1

Crystal data and refinement statistics.

Space group	C2
Cell dimensions	
a, b, c (Å)	199.3, 114.6, 74.3
β (°)	116.27
Z	4
Protein fraction (%)	39
Vm (Å^3/Da)	3.17
Total number of residues	862
Total nonhydrogen atoms	6914
Average temperature factors (Å^2)	
IFN-γ	44.5
IFN-γRα	
D1 of R1	58.7
D2 of R1	55.6
D1 of R2	58.0
D2 of R2	60.8
D1 of R3	115.3
D2 of R3	62.1
Resolution range of reflections used (Å)	6.0–2.9
Amplitude cutoff	None
R factor (%)	23.7
Free R factor (%)	30.2
Stereochemical ideality	
bonds (Å)	0.014
angles (°)	2.29
impropers (°)	1.93

structures determined by MAD phasing [17]. In addition, the phasing utilized only six selenium atom positions, which required extraction of a very weak anomalous signal (1 selenium/144 residues or 20 kDa/selenium atom). The large MAD structures reported to-date have utilized considerably stronger phasing signals, typically corresponding to 1.6 to 5.6 kDa per selenium atom [17].

In addition, the approach used here allowed the MAD analysis of a mixed complex in which one component was expressed in *E. coli* and contained selenium atoms, whereas the other component was glycosylated. This method of selenium incorporation may be particularly useful when different expression systems are required to produce the different components of a macromolecular assembly. Finally, the experiment utilized a protein of known structure containing selenium-substituted residues thereby allowing the use of molecular replacement methods to locate the selenium positions when the anomalous signal was weak. Critical to the success of this project was the combined use of efficient and sensitive CCD-based X-ray detectors, an intense, tunable synchrotron source and cryoprotection of the radiation-sensitive crystals.

Description of the overall structure

The asymmetric unit of the crystals contains three glycosylated IFN-γRα fragments, each consisting of the first 245 residues of the extracellular domain minus the 17-residue-long signal domain, and one non-glycosylated IFN-γ dimer, of which each IFN-γ chain consists of the first 133 residues plus an extra N-terminal methionine (Figure 1). Two of the glycosylated sIFN-γRα molecules (R1 and R2) are symmetrically bound to the IFN-γ dimer in the same way as previously reported for the 2:1 non-glycosylated receptor–ligand complex [7]. The two bound receptor chains do not interact, their closest distance being 30 Å. The third receptor molecule, R3, makes contacts with both R1 and R2, but not with IFN-γ. In principle, either of the two equivalent R3 molecules can be chosen to define a 3:1 complex. In either case the interactions involve primarily the C-terminal receptor domains. We have chosen the 3:1 complex involving R1–R3 interactions because it is more compact than the one involving R2–R3 interactions.

The presence of the third receptor domain was unexpected as the material used for crystallization had been purified and well characterized as a 2:1 complex [18]. Sodium dodecyl sulfate polyacrylamide gel electrophoresis (SDS–PAGE) of washed, redissolved crystals showed only intact ligand and receptor molecules (data not shown), but their relative amounts were not quantified. We can only speculate that during crystal growth, and perhaps favored by the specific crystallization conditions, partial dissociation of 2:1 complexes can take place to the extent needed for incorporation of an extra receptor molecule into the crystal lattice.

Structure of the IFN-γ homodimer

The IFN-γ homodimer is composed of two monomers (I1 and I2) that contain six α helices each. Four of the helices of one monomer are interdigitated with two of the helices of the other monomer thereby forming a globular structure with a noncrystallographic twofold axis. All 12 helices run approximately parallel to the local twofold axis. Both the

Figure 1

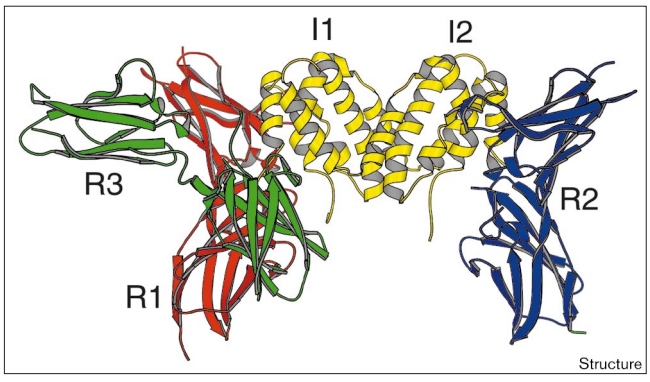

Ribbon diagram of the 3:1 sIFN-γRα–IFN-γ complex. The complex is formed by combining the 2:1 complex with receptor R3. The IFN-γ dimer (I1 and I2) is shown in yellow; the R1 receptor is in red, the R2 receptor in blue, and the R3 receptor in green. The complex is oriented such that the normal axis to the cell membrane is approximately vertical.

C-terminal tails are poorly ordered after residue 120. Weak continuous density is seen up to about residue 126 in both ligand chains but the structural model fitted to this density has very large refined B factors.

The α-helical IFN-γ structure is similar to that previously reported for both the free and bound forms [7,19]. The two IFN-γ monomers present in our structure are nearly identical. The largest differences are observed at the N and C termini; however, these regions are affected by high thermal parameters and structural disorder. The bound IFN-γ monomers differ most significantly from those of the free dimer in one loop region (residues 16–27) with deviations as large as 7.7 Å observed at residue 23. In the free form, this loop is somewhat disordered [19], but in the complex it becomes well ordered through the extensive interactions with the receptor, giving rise to the formation of a 3_{10} helix at residues 20–23 as previously described for the non-glycosylated 2:1 complex [7].

Structure of the glycosylated sIFN-γRα

The glycosylated sIFN-γRα molecule consists of two immunoglobulin-like β-sheet domains (D1 and D2 for the N- and C-terminal domains, respectively) each with fibronectin type-III topology (Figure 2a). The D1 and D2 domains are connected by a short, flexible linker. The D1 domain, composed of residues 14–102, forms a β sandwich with three β strands stacked on a layer of four β strands. The D2 domain, composed of residues 114–221, also forms a β sandwich; in this case both β sheets consist of four β strands. The 11-residue-long linker domain (residues 103–113) contains a six-residue helix that is also observed in human tissue factor [20].

In the final model, the two ligand-binding receptors R1 and R2 have residues missing in the loop connecting strands B and C of the D2 domain and at their disordered N and C termini.

Conformational variability of residues 131–139 of the BC loop has also been observed in the previously reported 2:1 complex [7]. The D2 domain of the third receptor, R3, is clearly visible in the electron-density maps. However, the entire D1 domain of R3 is highly disordered and only weak, non-contiguous electron density, consistent with the specific fold of D1, was observed in this region. The high degree of disorder observed for this domain is consistent with the observation that D1 of R3 is not involved in any intermolecular contacts in the crystal. Consequently, no conclusions have been drawn regarding the functional and structural roles of individual amino acid residues within the D1 domain of R3.

The structure of the glycosylated sIFN-γRα molecule reported here appears to be very similar to that of the molecule expressed without glycosylation, which has been described in detail [7]. However, detailed comparisons are not possible because the coordinates of the 2:1 non-glycosylated complex are unavailable. Within the 3:1 complex reported here, superposition of the D2 domains of the three crystallographically independent receptor chains shows that the relative orientations of domains D1 and D2 are nearly identical for R1 and R2, but appears quite different for R3 (Figure 2b). The hinge angle between D1 and D2 is ~120° for R1 and R2 but reduces to 110° for R3. Without such a change in the hinge angle, D1 of R3 would collide with neighboring molecules in the crystal. Neither the two D1 domains of R1 and R2 (that of R3 was treated as a rigid body) nor the three D2 domains show significant structural variation in this 2.9 Å structure, owing, in part, to the noncrystallographic symmetry restraints that were applied during refinement. Through inspection of difference maps, significant structural differences were indicated in the region of residues 164–170 and 218–220 and the restraints were correspondingly relaxed. The largest deviations are seen in poorly ordered loop regions, where some B factors are greater than 75 $Å^2$.

Glycosylation sites of sIFN-γRα

Each of the sIFN-γRα molecules contains four glycosylation sites, residues 17, 62, 69 and 162, all of which are asparagines. A fifth potential glycosylation site, Asn223, was shown to be unpopulated in the expression system used here [21]. The electron density of the sIFN-γRα–IFN-γ complex shows carbohydrate density at each of the four residues within R1 and R2. For the more disordered R3, only the glycosylation site of the D2 domain, Asn162, shows clear electron density. The electron density at these glycosylation sites typically extends for ~10 Å beyond the asparagine residues. The density at each site is weak relative to the protein density and forms a branching network, thus preventing detailed modeling. The density of the glycosylation site of Asn62 of R2 is shown in Figure 3. Glycosylation does not appear to be involved in either the receptor–ligand interactions or in any crystal contacts.

Receptor–ligand interactions

The 2:1 receptor–ligand complex has approximate twofold symmetry, and it is reasonable to assume that the membrane-inserted complex containing the full-length receptor would have this twofold axis oriented perpendicular to the membrane with the C terminus of the truncated receptor chains close to the membrane (see Figure 1). Each of these receptor chains forms a contiguous interface with the IFN-γ dimer, involving segments from both domains of the ligand. A detailed description of the receptor–ligand interactions for the previously reported structure determination of the 2:1 complex containing non-glycosylated sIFN-γRα molecules has been presented [7].

Overall, the interactions described by Walter *et al.* [7] are quite similar to those observed here, but as coordinates are

Figure 2

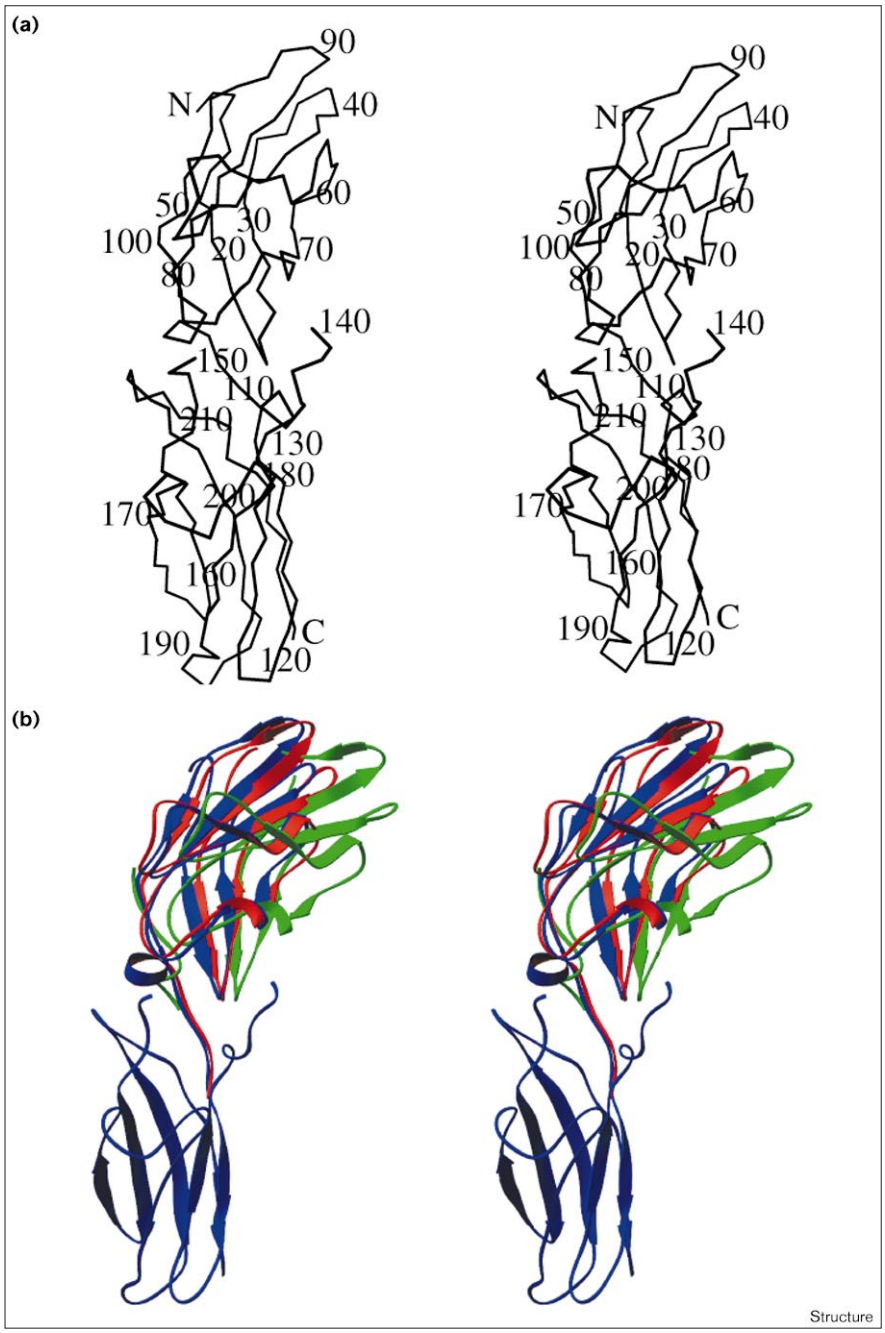

Structure of sIFN-γRα. **(a)** Stereoview Cα trace for sIFN-γRα with every tenth residue labeled. **(b)** Superposition of the three sIFN-γRα molecules. The superposition of the receptor molecules is based on the D2 domain only. Variations of the hinge angle between the D1 and D2 domains of each receptor is shown. The R1 receptor is in red, the R2 receptor in blue, and the R3 receptor in green.

not available no detailed comparison can be presented. The putative hydrogen-bonding interactions observed in the interface of our structure are listed in Table 2. Seven of the listed putative interactions, highlighted in bold, were not reported in the previous structure determination [7]. Mainchain hydrogen-bond interactions contribute significantly to the binding interface, and in both structures the receptor–ligand interactions appear highly symmetrical. One difference is the mainchain conformation at Gly18–His19, which in I2 leads to the formation of a hydrogen bond to the receptor Trp82 sidechain as in Walter *et al.* [7], while in I1 this peptide plane is rotated by ~90°. Closer examination of their stereochemistry and environment in both interfaces shows that the salt-bridge interaction of Lys12 with Glu101 and the Lys108–Tyr49 hydrogen bond nicely complement the previously reported interactions of the buried Glu101 and Tyr49 receptor sidechains. The Ala118–His205 hydrogen bond

Figure 3

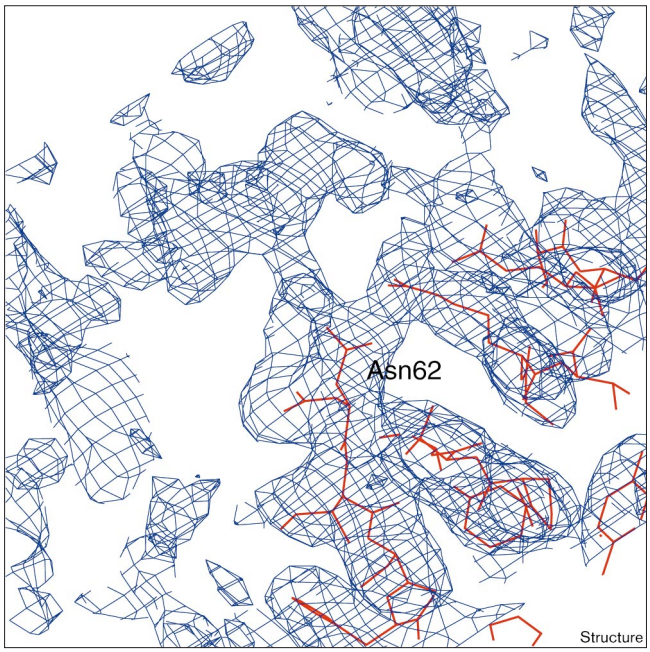

Electron density in the region of expected glycosylation. The final $2F_o–F_c$ map, contoured at 1.2σ, shows weak glycosylation density branching from Asn62 of the R2 receptor. Other potential glycosylation sites show similar electron density.

Table 2

Potential hydrogen-bond and salt-bridge interactions between the IFN-γ dimer and the sIFN-γRα molecules.

IFN-γ	sIFN-γRα	Distance (Å)
I1 Gln1 Nε2	R1 Trp207 O	2.6
I1 Glu9 Oε1	R1 Arg106 Nε	3.4
I1 Glu9 Oε1	**R1 Trp207 Nε1**	**3.0**
I1 Lys12 Nζ	**R1 Glu101 Oε1**	**2.9**
I1 Ser20 OH	**R1 Lys98 Nz**	**3.2**
I1 Ala23 O	R1 Gly50 N	3.3
I1 Ala23 O	R1 Val51 N	3.0
I1 Asp24 Oδ1	R1 Lys47 Nζ	2.6
I1 Asp24 Oδ1	**R1 Ser54 OH**	**2.8**
I1 Asn25 N	R1 Val51 O	3.3
I1 Asn25 N	**R1 Asn53 O**	**2.8**
I1 Gly26 N	R1 Val51 O	2.6
I1 Lys108 Nζ	**R2 Tyr49 OH**	**2.9**
I1 His111 Nε2	R2 Glu101 Oε1	2.8
I1 Glu112 Oε2	R2 Tyr49 OH	2.9
I1 Gln115 Nε2	R2 Asn79 Oδ1	2.9
I1 Ala118 O	**R2 His205 Nε2**	**3.0**
I2 Gln1 Nε2	R2 Trp207 O	3.2
I2 Glu9 Oε1	R2 Arg106 Nε	3.2
I2 Glu9 Oε1	**R2 Trp207 Nε1**	**3.5**
I2 Lys12 Nζ	**R2 Glu101 Oε1**	**3.0**
I2 Gly18 O	R2 Trp82 Nε1	3.0
I2 Ser20 OH	**R2 Lys98 Nζ**	**3.0**
I2 Ala23 O	R2 Gly50 N	3.1
I2 Ala23 O	R2 Val51 N	2.7
I2 Asp24 Oδ1	R2 Lys47 Nz	2.9
I1 Asp24 Oδ1	**R2 Ser54 OH**	**2.8**
I2 Asn25 N	R2 Val51 O	2.8
I2 Asn25 N	**R2 Asn53 O**	**2.9**
I2 Gly26 N	R2 Val51 O	2.6
I2 Lys108 Nζ	**R1 Tyr49 OH**	**3.2**
I2 His111 Nε2	R1 Glu101 Oε1	2.9
I2 Glu112 Oε2	R1 Tyr49 OH	2.8
I2 Gln115 Nε2	R1 Asn79 Oδ1	2.7
I2 Ala118 O	**R1 His205 Nε2**	**3.3**

Because of the resolution of the diffraction data and the error within the final structure, probable interactions separated by as much as 3.8 Å are listed. Interactions involving the C termini of the IFN-γ chains where B factors of the mainchain atoms exceed 100 Å^2 have been excluded. Those interactions not reported in Walter *et al.* [7] are in bold type.

also shows good stereochemistry in both interfaces. The remaining four newly reported interactions (Glu9–Trp207, Ser20–Lys98, Asp24–Ser54, Asn25–Asn53) suffer from unfavorable stereochemistry.

Studies with C-terminally truncated IFN-γ variants have shown that in the C terminus, in particular, the highly basic segment Lys128–Arg129–Lys130–Arg131 contributes significantly to binding [22,23]. However, it has remained controversial whether this is due to specific ligand–receptor interactions or to other structural effects [24]. No interactions were reported beyond residue 115 of IFN-γ in the 2:1 complex and the authors suggested that a plausible interaction with an acidic cluster on the receptor chain might have been prevented by crystal contacts [7]. In our structure, the electron density is weak beyond residue 120 of IFN-γ and the twofold symmetry is no longer preserved. Although models were built and refined up to residue 126, they are not reliable for this segment, as indicated by very high thermal parameters. The modeled conformations with the Lys125 sidechains interacting with Glu173 and/or Glu175 for I1 and with Glu180 for I2 at best represent partially populated conformational states. However, the interactions with the acidic cluster on the receptor chains are not hindered by crystal contacts. It appears that the contribution of the C-terminal tails to receptor binding is not through a structurally defined, specific interface. It cannot be ruled out, however, that nonspecific interactions between the basic and acidic clusters on IFN-γ and its receptor, respectively, involving multiple conformational states, account for the observed binding contribution of the C terminus.

Receptor–receptor interactions in the crystal packing

Crystals of the glycosylated complex generally displayed anisotropic diffraction falling off in the direction corresponding to the c axis. Examination of the crystal contacts reveals that the third receptor molecule R3 plays an important role in mediating intermolecular contacts along this axis. In the current structure (Figure 4), the D2 domains of the symmetry-related R2 receptor chains form crystal-packing contacts. The R1 molecules are not linked to each

other through crystal-packing contacts. Instead, the D2 domain of R1 and a symmetry-related D2 domain of R2 are bridged by the D2 domain of R3 (Figure 4a). The contacts along c are thus mediated by three distinct interfaces, each of which involves two D2 receptor domains (R2/R2′, R3/R1 and R3/R2). Moreover, all three contacts involve β strand C′ from at least one of the D2 domains. These interactions are listed in Table 3. Two of the β-strand interactions are antiparallel (R2–R2′ and R3–R2) whereas the third is parallel (R3–R1). The antiparallel R2–R2′ interaction between two symmetry-related C′ strands involves four hydrogen bonds between mainchain atoms and four hydrogen bonds between sidechain atoms. The antiparallel R3–R2 interaction is between strand C′ on R3 and strands A and G on R2. Two hydrogen bonds between mainchain atoms and three more potential hydrogen bonds involving sidechain atoms are observed. The parallel R3–R1 interaction is between strands A and G on R3 and strand C′ on R1. Four mainchain hydrogen bonds, three hydrogen bonds involving sidechain atoms and one salt bridge are observed in this interface.

We have examined a number of crystal structures containing structurally homologous cytokine receptors for the occurrence of similar interdomain contacts. We could not find any additional examples of receptor molecules that are involved in analogous interactions.

The observed receptor–receptor interactions may reflect the tendency for receptor domains to associate and has prompted us to examine whether such interactions could mimic the association of the 2:1 complex with the structurally homologous Rβ chain [15]. Ternary complex formation of IFN-γ with the Rα and Rβ receptors has been shown to occur on the cell surface and, using truncated extracellular receptor domains, also in solution [2]. Although it has not been demonstrated experimentally, we consider it probable that Rβ interacts with both IFN-γ and Rα in the ternary complex. No binding of Rβ to either Rα or IFN-γ alone has been reported and the individual, putative interfaces most probably provide only little

Figure 4

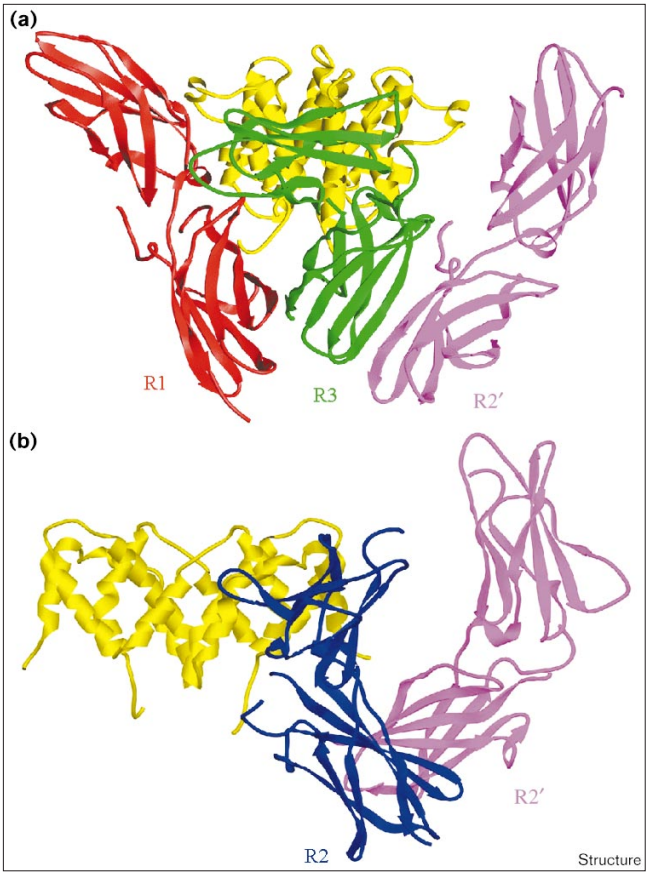

Crystal contacts involving D2 receptor domains. **(a)** Receptor R3 is shown in green bridging receptor R1 (red) and a symmetry-related receptor R2′ (magenta). **(b)** Receptor R2 is shown in blue and an R2 receptor related by twofold symmetry (R2′) is shown in magenta. These interactions form the primary packing contacts in the crystals of the complex.

Table 3

Potential hydrogen-bond and salt-bridge interactions in receptor–receptor contacts.

Interaction		Distance (Å)
Parallel strand interaction between R1 and R3		
R1	R3	
Glu165 O	Glu216 N	3.8
Gln167 N	Glu216 O	3.1
Gln167 O	Cys218 N	3.3
Tyr168 OH	Gln195 Oδ1	3.3
Lys169 Nζ	Asp116 Oδ1	2.9
Lys169 N	Cys218 O	3.5
Lys174 Nζ	Lys119 O	2.6
Ala186 O	Gln195 Nε2	3.1
Antiparallel strand interaction between R3 and R2		
R3	R2′	
Gly163 O	Lys119 Nζ	3.8
Glu165 O	Thr220 N	2.5
Gln167 N	Cys218 O	3.8
Tyr168 OH	Asp116 Oδ1	3.8
Ser191 Oγ	Lys119 O	2.4
Antiparallel strand interaction between R2 and R2′		
R2	R2′	
Glu165 Oε1	Lys169 Nζ	3.3
Glu165 O	Lys169 N	3.6
Gln167 N	Gln167 O	3.3
Gln167 Oε1	Gln167 Nε2	3.4
Gln167 Nε2	Gln167 Oε1	3.4
Gln167 O	Gln167 N	3.3
Lys169 N	Glu165 O	3.6
Lys169 Nζ	Glu165 Oε1	3.3

Because of the resolution of the diffraction data and the error within the final structure, likely interactions separated by as much as 3.8 Å are listed.

binding energy. Furthermore, the location of the ternary complex on the cell surface produces topological constraints for plausible ternary complex structures. In particular, the C termini of the associated Rα and Rβ receptor chains should be close to a plane located on one side of the complex and approximately perpendicular to the twofold axis of the 2:1 complex (Figure 1). Only one of the three observed Rα–Rα interactions, the parallel strand interaction R3–R1, is compatible with this constraint. Interestingly, the D1 domain of R3 is positioned such that interactions of the third receptor with the cytokine ligand appear possible. Figure 5 shows the atomic interactions that form the parallel β-sheet interaction between R1 and R3 resulting in the 3:1 complex shown in Figure 1.

The 3:1 complex suggests a structural model that may provide insight into the formation of the ternary complex in the IFN-γ signaling pathway. Although the third receptor may be only an artifact of crystallization, it is nevertheless interesting to speculate about the implications for association of the Rα and Rβ chains with the IFN-γ ligand. Because the Rα and Rβ chains showed significant homology, we believe that the Rα chain is a reasonable model for Rβ [2,3]. In modeling the ternary complex, the positioning of the third Rα chain in this 3:1 complex reveals that only the domain 2 region of the third receptor could make contact with the IFN-γ ligand. In particular, the region between the end of strand C′ and the beginning of strand E, which is likely to assume a somewhat different structure in Rβ, lies close to the N terminus and to helix D of IFN-γ. In addition, the model could accommodate an additional twofold-related Rβ giving an overall stoichiometry of 2:2:1. Although addition of this final Rβ molecule is prevented by crystal packing, it could be easily accommodated in the isolated IFN receptor complex. In fact, it is difficult to imagine other ways that a symmetric 2:2:1 complex, in which receptors interact through their C-terminal domains, could be formed. Obviously this model is very speculative and an experimentally determined structure of the ternary complex of IFN-γ, Rα and Rβ is required to determine the detailed interactions. Nevertheless, our model makes some clear predictions that could be tested by further experimentation.

Figure 5

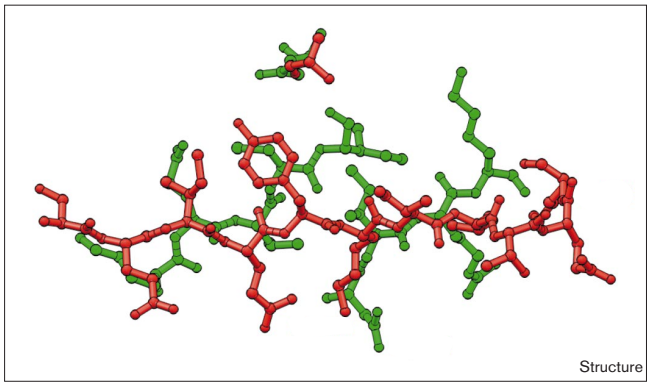

The R3–R1 parallel β-sheet interface. The portion of the interface consisting of R1 residues is shown in red and that of R3 is in green. Key residues are labeled.

Biological implications

Protein–protein interactions are ubiquitous in the biology of the cell. Here, we report new interactions in the 3:1 complex of the soluble portion of the high-affinity interferon-γ (IFN-γ) receptor bound to IFN-γ. The association of these two proteins is known to be the first step in the signaling pathway of the cell-secreted cytokine IFN-γ. For these studies, glycosylation was maintained on the receptor fragments. X-ray crystallography reveals the receptor–ligand association previously observed in a 2:1 non-glycosylated complex [7], but with a third receptor molecule present. Interactions involving the third receptor consist of contacts between β strands of the C-terminal domains of the receptor fragments. We believe the association of a third high-affinity receptor within the 3:1 complex suggests a model for higher order oligomerization. In particular, the binding of the third receptor may mimic the interaction of the accessory factor protein known to be required in the formation of the active IFN-γ signaling complex. It may also serve as a model for other cytokine signaling pathways for which receptor oligomerization occurs. The structure of the 3:1 complex reveals additional interactions within the receptor–ligand interface, thereby leading to a more complete description of this protein–protein interaction. Although glycosylation is evident in the crystal structure, it does not appear to be directly involved in any of the observed protein–protein interactions.

Materials and methods

Protein purification and crystallization

The extracellular domain (the 245 N-terminal residues minus the 17-residue-long N terminus signal domain) of the IFN-γRα chain was expressed in baculovirus-infected SF9 insect cells and was heterogeneously glycosylated. The molecular weight of the purified receptor fragment is 29 kDa, of which ~6 kDa are the carbohydrate moieties [18]. Human IFN-γΔ10 (lacking ten C-terminal residues) was expressed in *E. coli* and purified as a 32 kDa dimer as previously described [14]. In addition, SeMet-substituted IFN-γ was prepared for the MAD phasing experiment using an *E. coli* strain that is auxotrophic for methionine [14]. An extra methionine is present at the N terminus of each monomer in *E. coli*-derived IFN-γ. The receptor–ligand complex of the native IFN-γ was formed and characterized by chemical cross-linking, chromatography, analytical centrifugation and laser-light scattering [25]. These results suggest that two sIFN-γRα were bound to each IFN-γ dimer. Similar procedures were followed in the formation of the complex containing SeMet IFN-γ. The SeMet complex contained eight SeMet residues.

Native and SeMet complexes were crystallized in a pH 7.0 solution containing 12.5% PEG 8000 and Tris buffer by the hanging-drop method as previously described [16]. The native and the SeMet-incorporated complexes behaved similarly and crystallized in the monoclinic space

group, C2, resulting in small plate-like crystals. The sIFN-γRα–IFN-γ crystals diffract weakly with mosaic spreads in excess of 1° and exhibited severe radiation damage. The unit-cell dimensions of the native crystal form were a = 199.30 Å, b = 114.65 Å, c = 74.34 Å, and β = 116.27°, while those of the SeMet-incorporated complex were a = 201.51 Å, b = 113.90 Å, c = 74.10 Å, and β = 117.04°. The crystals contain one 120 kDa complex in the asymmetric unit resulting in 61% solvent content.

X-ray data collection

The MAD data were collected at the Cornell High Energy Synchrotron Source (CHESS) using station F2 and a 1k × 1k CCD-based X-ray detector, with an active area of 52 mm × 52 mm [26]. Data were collected at four X-ray wavelengths near the Se K-edge corresponding to the most negative value of f′ (λ_1 = 0.9795 Å), the maximum value of f″ (λ_2 = 0.9793 Å), intermediate values of f′ and f″ (λ_3 = 0.9790 Å), and a remote reference wavelength (λ_4 = 0.9642 Å). The Bijvoet pairs were measured using inverse-beam geometry. The intensity of the F2 beam was low because of monochromator heating, resulting in long exposure times of 5–10 min per 2° oscillation. In addition to being unusually weak, the diffraction from these crystals was highly anisotropic and extended to only 3.8 Å resolution for the SeMet complex. Even with liquid-nitrogen-cooling, the crystals were radiation-sensitive and four crystals were required to obtain a complete MAD data set. The data from each crystal were processed independently using the computer program DENZO [27]. Merging and scaling was compromised by lack of overlap among the four different crystals. Using the native data set described below, each MAD data set was brought to a common scale with anisotropic scaling using the program SCALEIT [28]. The combined MAD data was 75% complete to 3.8 Å resolution. The data collection and processing statistics for the four Se-Met crystals are given in Table 4.

Higher resolution diffraction was observed from native IFN-γRα–IFN-γ crystals using the high intensity A-1 wiggler stations at CHESS. A data set extending to 2.7 Å was measured (λ = 0.919 Å) using a 2k × 2k CCD-based X-ray detector with an active area of a 82 mm × 82 mm [29] and a single flash-cooled native crystal. Diffraction from this crystal was isotropic and stronger than the crystals used for MAD data, resulting in exposure times of 60 s per 1° oscillation. The native crystal had a mosaicity of approximately 1°. The native data were processed using the computer program DENZO [27]. The data collection and processing statistics for the native crystal are given in Table 4.

Structure determination

Initial attempts to determine the positions of the selenium atoms from the inspection of the Patterson map were unsuccessful. Therefore, the previously determined unbound IFN-γ dimer structure [19] was oriented and positioned in the crystal coordinate system using the molecular replacement program AMoRe [29]. Phases were calculated from the IFN-γ model (27% of the total asymmetric unit) and model bias was removed using SIGMAA [29]. A difference Fourier map was calculated using the weighted molecular replacement phases and the coefficients corresponding to SeMet-incorporated complex data minus the native data. The top four peaks corresponded to known methionine residues of the IFN-γ, with two of these peaks falling in the region of each IFN-γ monomer where two neighboring methionines are difficult to distinguish from each other at this resolution. Therefore, the six sulfur sites of the native IFN-γ were used as initial estimates of the selenium atom positions for subsequent MAD phasing. The two N-terminal methionines unique to the *E. coli*-derived IFN-γ appeared to be disordered. The six selenium atom positions were used to calculate phases using the program MLPHARE [29]. The initial 3.8 Å map showed the boundary of the complex and some features of the IFN-γ and the IFN-γ-bound sIFN-γRα molecules.

Phases were improved and extended to 2.7 Å using solvent-flattening, noncrystallographic symmetry (NCS) averaging, histogram matching and the program DM [29]. The resulting map allowed the building of partial models for the two ligand-bound sIFN-γRα molecules. The model, consisting of the IFN-γ dimer and the two sIFN-γRα chains, was initially refined against the diffraction data between 8.0 Å and 2.9 Å using the positional refinement of X-PLOR [30]. A randomly chosen set of 5% of the reflections were reserved for calculating the R_{free} value that was used as a guide throughout the refinement process. As the model was being built, three NCS operations were independently defined for I1 and I2, the D1 domains of R1 and R2, and the D2 domains of R1 and R2. The orientation matrix for each of these domains differed slightly. Updated solvent-flattening and averaging masks were frequently created as the model progressed.

After several iterative cycles of density modification and phase combination followed by further model building and positional refinement, an additional β-sheet domain became apparent in the electron-density maps. This surprising finding gave the first suggestion that a third sIFN-γRα molecule was present in the complex. Model building of the unexpected

Table 4

Statistics of the X-ray diffraction data.

Crystal	Exposure time (s)	Resolution (Å)	Wavelength (Å)	Measured reflections	Unique reflections	Completeness (%)	R_{sym}*	R_{iso}†
1	300	20–3.8	0.9795	28,459	9919	34.3	0.059	0.216
			0.9793	28,473	9866	34.1	0.060	0.216
			0.9790	28,524	9896	34.2	0.060	0.216
			0.9642	28,444	9815	33.9	0.058	0.217
2	450–600	20–3.8	0.9795	40,128	11,043	38.2	0.074	0.275
			0.9793	40,198	11,063	38.2	0.074	0.273
			0.9790	40,150	11,031	38.1	0.076	0.275
			0.9642	40,087	11,070	38.3	0.076	0.276
3	600	20–4.0	0.9795	32,468	6366	25.7	0.092	0.251
			0.9793	32,525	6347	25.6	0.098	0.249
			0.9790	32,534	6392	25.8	0.093	0.252
			0.9642	32,034	6229	25.1	0.091	0.254
4	300–600	20–3.8	0.9795	38,768	9508	32.9	0.066	0.281
			0.9793	38,774	9516	32.9	0.067	0.282
			0.9790	38,804	9482	32.8	0.068	0.282
			0.9642	38,861	9457	32.7	0.067	0.286
Native	60	45–2.7	0.910	176,010	33,105	80.1	0.056	–

*$R_{sym} = \Sigma_{hkl} \Sigma_i |I_{hkl,i} - \langle I \rangle_{hkl}| / \Sigma |\langle I \rangle_{hkl}|$. †$R_{iso} = \Sigma | F_{PH} - F_P | / \Sigma F_P$.

electron-density domain produced a seven-stranded β-sheet sandwich structure. The identity of the region was determined crystallographically by aligning the modeled domain with the D1 and D2 domains of the two sIFN-γRα molecules. A high correlation was found with a particular orientation of one of the D2 domains. This alignment was then compared to the density-modified F_o map and striking agreement was found in the location of the disulfide bridges and various hydrophobic residues thereby confirming the assignment of the domain as a sIFN-γRα D2 domain.

Attempts to define the D1 domain of R3 were less convincing. A fourth NCS operation was defined relating the D2 domains of R2 and R3 in the final application of density modification. Also, a new protein mask was prepared for the entire complex by using the well defined D2 domain of R3 and an intact sIFN-γRα molecule to define the mask for D1 of R3. The calculated phases based on the existing model (not including D1 of R3) were combined with the MAD phases and the processes of solvent-flattening, histogram mapping and symmetry-averaging were again carried out. The resulting phases produced a map that suggested the placement of the D1 domain. The electron density in this region of the map, however, was not continuous. The D1 domain for R3 was positioned as a rigid body resulting in no bad contacts.

Several additional rounds of model adjustment and NCS-restrained positional refinement were conducted in which the atoms of the D1 domain of R3 were treated as a rigid body. The NCS restraints for specific residues were relaxed as the difference maps produced convincing indications that these residues with differing molecular contacts should have positional variations. Bulk-solvent modeling was not included because, on the basis of the R_{free} parameter, it failed to improve the refinement. Instead, somewhat lower R_{free} values were obtained when the model was refined against the data with a low-resolution cutoff of 6 Å rather than 8 Å. This was substantiated by control calculations in which R factors were calculated to only 6 Å for models refined against data extending to 8 Å. The results of the refinement are summarized in Table 1.

Accession numbers

The atomic coordinates have been deposited in the Protein Data Bank, operated by the Research Collaboratory for Structural Bioinformatics, with accession code 1FG9.

Acknowledgements

This work was conducted at CHESS, which is supported by the National Science Foundation (DMR-9311772), using the MacCHESS facility supported by the National Institutes of Health (RR-01646). The authors would like to acknowledge the support of the WM Keck Laboratory for Molecular Structure and the Lucille P Markey Charitable Trust. We thank Leslie Kinsland and Marian Szebenyi for assistance in the preparation of figures.

References

1. Bazan, J.F. (1990). Structural design and molecular evolution of a cytokine receptor superfamily. *Proc. Natl Acad. Sci. USA* **87**, 6934 6938.
2. Marsters, S.A., Pennica, D., Bach, E., Schreiber, R.D. & Ashkenazi, A. (1995). Interferon γ signals via a high-affinity multisubunit receptor complex that contains two types of polypeptide chain. *Proc. Natl Acad. Sci. USA* **92**, 5401-5405.
3. Bach, E.A., *et al*., & Schreiber, R.D. (1996). Ligand-induced assembly and activation of the γ interferon receptor in intact cells. *Mol. Cell Biol.* **16**, 3214-3221.
4. Wu, H., Kwong, P.D. & Hendrickson, W.A. (1997). Dimeric association and segmental variability in the structure of human CD4. *Nature* **387**, 527-530.
5. de Vos, A.M., Ultsch, M. & Kossiakoff, A.A. (1992). Human growth hormone and extracellular domain of its receptor: crystal structure of the complex. *Science* **255,** 306-312**.**
6. Somers, W., Ultsch M., de Vos, A.M. & Kossiakoff, A.A. (1994). The X-ray structure of a growth hormone-prolactin receptor complex. *Nature* **372**, 478-481.
7. Walter, M.R., *et al*., & Narula, S.K. (1995). Crystal structure of a complex between interferon-γ and its soluble high-affinity receptor. *Nature* **376**, 230-235.
8. Banner, D.W., *et al*., & Kirchhofer, D. (1996). The crystal structure of the complex of blood coagulation factor VIIa with soluble tissue factor. *Nature* **380**, 41-46.
9. Livnah, O., *et al*., & Wilson, I.A. (1996). Functional mimicry of a protein hormone by a peptide agonist: the EPO receptor complex at 2.8 Å. *Science* **273**, 464-471.
10. Vigers, G.P., Anderson, L.J., Caffes, P. & Brandhuber, B.J. (1997). Crystal structure of the type-I interleukin-1 receptor complexed with interleukin-1β. *Nature* **386**, 190-194.
11. Schreuder, H., *et al*., & Barrett, R.W. (1997). A new cytokine-receptor binding mode revealed by the crystal structure of the IL-1 receptor with an antagonist. *Nature* **386**, 194-200.
12. Christinger, H.W., *et al*., & de Vos, A.M. (1998). Crystallization of ovine placental lactogen in a 1:2 complex with the extracellular domain of the rat prolactin receptor. *Acta Crystallogr. D* **54**, 1408-1411.
13. Randal, M. & Kossiakoff, A.A. (1998). Crystallization and preliminary X-ray analysis of a 1:1 complex between a designed monomeric interferon-γ and its soluble receptor. *Protein Sci.* **7**, 1057-1060.
14. Dobeli, H., Gentz, R., Jucker, W., Garotta, G., Hartmann, D.W., & Hochuli, E. (1988). Role of the carboxy-terminal sequence on the biological activity of human immune interferon (IFN-γ). *J. Biotech.* **7**, 199-216.
15. Soh, J., *et al*., & Pestka, S. (1994). Identification and sequence of an accessory factor required for activation of the human interferon γ receptor. *Cell* **76**, 793-802.
16. Chene, C., Fountoulakis, M., Dobeli, H., D'Arcy, B., Winkler, F. & D'Arcy, A. (1995). Crystallization of the complex of human IFN-γ and the extracellular domain of the IFN-γ receptor. *Proteins* **23**, 591-594.
17. Deacon, A.M. & Ealick, S.E. (1999). Selenium-based MAD phasing: setting the sites on larger structures. *Structure* **7**, R161-R166.
18. Fountoulakis M., Takacs-di Lorenzo, E., Juranville, J.F., & Manneberg, M. (1993). Purification of interferon γ-interferon γ receptor complexes preparative electrophoresis on native gels. *Anal. Biochem.* **208**, 270-276.
19. Ealick, S.E., *et al*., & Bugg, C.E. (1991). Three-dimensional structure of recombinant human interferon-γ. *Science* **252**, 698-702.
20. Harlos, K., *et al*., & Boys, C.W.G. (1994). Crystal structure of the extracellular region of human tissue factor. *Nature* **370**, 662-666.
21. Manneberg, M., Friedlein, A., Kurth, H., Lahm, H.W., & Fountoulakis, M. (1994). Structural analysis and localization of the carbohydrate moieties of a soluble human interferon γ receptor produced in baculovirus-infected insect cells. *Protein Sci.* **3**, 30-38.
22. Haelewyn, J., Michiels, L., Verhaert, P., Hoylaerts, M.F., Witters R., & De Ley, M. (1997). Interaction of truncated human interferon gamma variants with the interferon gamma receptor: crucial importance of Arg129. *Biochem. J.* **324**, 591-595.
23. Lundell, D., *et al*., & Narula, S. (1991). The carboxyl-terminal region of human interferon γ is important for biological activity: mutagenic and NMR analysis. *Protein Eng.* **4**, 335-341.
24. Wetzel, R., Perry, L.J., Veilleux, C., & Chang, G. (1990). Mutational analysis of the C-terminus of human interferon-γ. *Protein Eng.* **3**, 611-623.
25. Fountoulakis M., Zulauf, M., Lustig, A., & Garotta, G. (1992). Stoichiometry of interaction between interferon γ and its receptor. *Eur. J. Biochem.* **208**, 781-787.
26. Tate, M.W., Eikenberry, E.F., Barna, S.L., Wall, M.E., Lowrance, J.L. & Gruner, S.M. (1995). A large-format high-resolution area X-ray detector based on a fiber optically bonded charge-coupled device (CCD). *J. Appl. Crystallogr.* **28**, 196-205.
27. Otwinowski, Z. (1991). Processing of X-ray diffraction data collected in oscillation mode. *Methods Enzymol.* **276**, 307-326.
28. *CCP4 Collaborative Computational Project, Number 4*. (1994). The CCP4 suite: programs for protein crystallography. *Acta Crystallogr. D* **50**, 760-763.
29. Thiel, D.J., Ealick, S.E., Tate, M.W., Gruner, S.M. & Eikenberry, E.F. (1996). Macromolecular crystallographic results obtained using a 2048 × 2048 CCD detector at CHESS. *Rev. Sci. Instrum.* **67**, 3361-3364.
30. Brünger, A.T. (1992). *X-PLOR, A system for X-ray Crystallography and NMR*. Yale University Press, New Haven, CT, USA.